Thermal Boundary Layers in Sweeping Gas Membrane Distillation Processes

M. Khayet, M. P. Godino, and J. I. Mengual
Dept. of Applied Physics I, University Complutense of Madrid, 28040 Madrid, Spain

The sweeping gas membrane distillation process was analyzed in a plate and frame membrane module, and a method clarifying the contribution of each boundary layer separately was developed. The temperature polarization coefficients of the fluid phases as well as the overall one have been defined, and their effects on the permeate flux were studied. Also studied is the influence of experimentally relevant parameters, such as the inlet temperatures or circulation velocities of the fluids. Results from two porous and hydrophobic membranes in different experimental conditions were interpreted on the basis of a combined Knudsen/molecular diffusion flow model. The theory agreed well with the experiment.

Introduction

The process called membrane distillation (MD), which has been known since the late 1960s, refers to the thermally driven transport of water vapor through a porous hydrophobic partition (Lawson and Lloyd, 1997). In the former contributions, a membrane was placed between two aqueous solutions, giving rise to the experimental configuration termed direct-contact membrane distillation (DCMD). The transport is due to the hydrophobicity of the membrane material, as the liquid water cannot enter the pores unless a hydrostatic pressure, exceeding the so-called "liquid entry pressure of water (LEP_w)" is applied (Sarti et al., 1985; Peña et al., 1993). In the absence of such a pressure difference, a liquid–vapor interface is formed on either side of the membrane pores. If a temperature difference is maintained through the membrane, a water-vapor pressure difference appears. Consequently, water molecules evaporate at the hot interface, cross the membrane in the vapor phase, and condense in the cold side, giving rise to a net transmembrane water flux.

The MD process can be carried out with other experimental configurations depending on the method by which the water vapor is recovered from the pores (Lawson and Lloyd, 1997): air-gap membrane distillation (AGMD), sweeping gas membrane distillation (SGMD), and vacuum membrane distillation (VMD). In AGMD, there is a stagnant air gap plus a cold metallic plate on which the transported vapor is condensed in place of the cold liquid chamber. In SGMD, the water vapor is swept by a collecting gas and then condensed out of the membrane module. Finally, in a VMD configuration, the water vapor is removed with the help of a vacuum system and then collected in cold traps. Each one of these possibilities has its advantages and inconveniences and has been used in different cases. An examination of the literature shows that the DCMD has been the most frequently considered configuration (Drioli and Wu, 1985; Franken et al., 1987; Chmielewski et al., 1995; Gryta and Tomaszewska, 1998; Vázquez-González and Martínez, 1994). In contrast, very little work has been done in the field of SGMD (Basini et al., 1987; Khayet et al., 2000a,b). This is probably due to the fact that the transported water must be collected in an external condenser, and this implies an extra step. Nevertheless, if one considers that the SGMD configuration combines a relatively low conductive heat loss with a reduced mass-transfer resistance, the perspectives for the future sound interesting.

The simultaneous heat and mass transfer taking place through the membrane create thermal gradients in the fluid phases adjoining the membrane surface. In this way, the effective driving force is lower than expected. This phenomenon is called "temperature polarization (TP)" (Schofield et al., 1987). Different theoretical approaches, which correspond to the different experimental configurations, have been proposed to evaluate the importance of the TP effects (Lawson and Lloyd, 1997; Khayet et al., 2000a,b; Schofield et al., 1987; Ortiz de Zárate et al., 1990; Godino et al., 1996). In most of the MD references reported in Lawson and Lloyd (1997), particularly in the DCMD and AGMD modes, the TP effects are supposed to be similar on both sides of the membrane in spite of the fact that the adjoining fluids have different physicochemical properties.

Correspondence concerning this article should be addressed to J. I. Mengual.

In previous articles (Khayet et al., 2000a,b), the SGMD configuration has been studied with the help of a theoretical approach that is based on the TP effects and on the mechanisms of heat and mass transfer. Based on this model, in the present article we propose a method that permits consideration of the TP effects, taking into account the asymmetric properties of the fluids (a hot liquid and a cold sweeping gas). As far as we know, this is the first time that such a study has been carried out in the field of MD. Some experiments have been developed in a plate and frame membrane module, with pure water as the hot liquid feed and water-saturated air as the cold sweeping gas. The experiments mainly study the role of relevant parameters, such as the inlet and outlet temperatures and the circulation velocities of both fluids. Two commercial membranes were used. The experimental results are discussed on the basis of the theoretical model and the agreement can be considered good.

Experimental Studies

Materials

Experimental tests were conducted with two commercial porous hydrophobic flat-sheet membranes: the TF-200 and TF-450, both supplied by Gelman Science Inc. These membranes are made of polytetrafluoroethylene (PTFE), supported by a polypropylene net. Their principal characteristics, as specified by the manufacturer, are as follows:

- TF-200: pore diameter 0.2 μm; thickness 178 μm; fractional void volume 80%; liquid entry pressure of water 281.7 kPa.
- TF-450: pore diameter 0.45 μm; thickness 178 μm; fractional void volume 80%; liquid entry pressure of water 137.8 kPa.

Pure water (deionized and distilled) and air were employed.

Apparatus

The experimental device used can be seen in Figure 1. The central part consists of a plate and frame Filtron Minisette membrane module, supplied by Gelman Science Inc. and modified according to our requirements. Basically, it consists of two flat chambers made with silicone separators placed between two acrylic manifolds. The membrane was fixed between the chambers, having an effective area of about 56×10^{-4} m^2. The hot liquid water and the cold air were flowed tangentially at both sides of the membrane, in a countercurrent mode, to improve the driving force. The remainder of the experimental device consisted of a graduated glass container to store the liquid feed and to measure the temporal evolution of the feed level.

The temperatures of the liquid feed and of the sweeping air were measured continuously at the inlet and at the outlet of the membrane module. These temperatures were measured in steady state with Pt100 probes connected to a digital multimeter AMR 3280-6, with an accuracy of ± 0.1°C. In order to avoid the membrane wetting, the pressure gradient through the membrane was controlled with two manometers (Wika; ± 0.05 bar) placed at the inlets of the module.

The liquid feed was circulated by a peristaltic pump Masterflex 7549-40, and its flow was measured with a Tecfluid

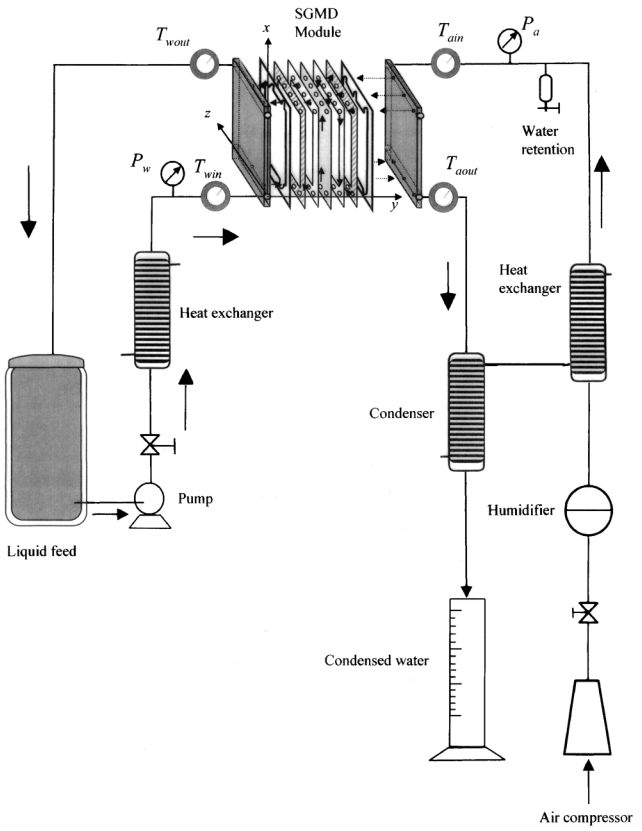

Figure 1. Experimental device.

6001 flowmeter, with a precision of $\pm 2\%$. For experimental reasons, the temperature of the liquid was controlled with the help of a heat exchanger connected to a thermostat located between the pump and the membrane module. The sweeping gas flow was maintained with a Fiac 1001 compressor. A humidifier might be incorporated to induce the water saturation of the air. The air flow was measured with a Gilmont 51552 flowmeter, with a precision of $\pm 3\%$. A cooling thermostat Techne RB-12A was used to control the temperature of the air and to induce the condensation of the distilled water by means of two heat exchangers located at the entrance and exit of the cold-air side of the membrane module. A graduated cylinder was used to collect directly the distilled water from the outlet port of the condenser. In order to reduce the energy losses to the surroundings, the membrane module, the container, and the pipes were thermally isolated.

Experiments

The setup just described permits liquid water and sweeping air to be circulated separately at each side of the membrane module. The MD flux was measured under different conditions of the circulation velocity and inlet temperature of both fluids. It is worth pointing out that the circulation velocity of the fluids must be varied with due precautions, in order to avoid membrane wetting. This implies that two conditions must be fulfilled: (1) the pressure difference between the fluids must be lower than the LEP_w, and (2) the air pressure

must be lower than the liquid pressure. With this in mind, the circulation velocity of the sweeping air was varied between 0.4 and 2.0 m/s, and its inlet temperature was varied between 10 and 30°C. Similarly, in the case of the liquid feed the ranges were between 0.07 and 0.21 m/s for the circulation velocity, and between 40 and 70°C, for the inlet temperature. In order to assure the absence of membrane wetting, the electrical conductivity of the distillate at the end of each set of experiments was measured with a sodium chloride aqueous solution of 1 M as the feed and a 712-Ω Metrohm conductivimeter.

The flux of distilled water was calculated in every case by measuring the volume every 10 min for 3 h, and adjusting the experimental pairs of data {volume−time} to a straight line by a least-square method. The correlation coefficient was always better than 0.99, which means that the procedure is adequate. This procedure was carried out in both hot and cold chambers, and the agreement was good ($\pm 2\%$). In order to assure that the water fluxes measured in both chambers were equal, the distillate was condensed at the same temperature at which the saturated sweeping air entered the module.

Theoretical Approach

The system to be studied consists of a porous hydrophobic membrane, which is held between two chambers. Hot pure water is circulated through one of the chambers and cold sweeping air is circulated through the other. This situation corresponds to the embodiment known as SGMD. The hot water and the cold sweeping gas counterflow tangentially to the membrane surfaces in a plate and frame membrane module. The temperature difference gives rise to a water-vapor pressure difference and, consequently, to a transmembrane water flux (N).

The MD flux, N, is affected by the presence of boundary layers at both sides of the membrane (by the existence of TP effects). These effects will be discussed more fully later. As a consequence, N can be written as a function of the transmembrane water-vapor pressure difference, $\Delta P'_v$, or of the value corresponding to the bulk phases, ΔP_v

$$N = B\Delta P_v = B'\Delta P'_v \tag{1}$$

where B and B' are the overall and net MD coefficients, respectively. These coefficients depend on membrane characteristics (membrane thickness, tortuosity, etc.), as well as on different experimental parameters (temperature, pressure, etc.).

According to Lawson and Lloyd (1997), Khayet et al. (2000b), and Schofield et al. (1990), the MD flux can be explained in the framework of different transport models: the Knudsen model, the Poiseuille model, the molecular diffusion model and/or the combinations among them. Determination of the best model depends on the relative magnitudes of the pore size and of the mean free path of the water molecules inside the pores. In Khayet et al. (2000b) this problem was analyzed in SGMD processes, and it was concluded that the vapor transport takes place via a combined Knudsen/molecular diffusion mechanism. In this case, the net MD coefficient may be written as

$$B' = \frac{M}{RT}\left(\frac{1}{D_K} + \frac{P_a}{D_M}\right)^{-1}\frac{1}{\delta} \tag{2}$$

where P_a is the pressure of the air entrapped in the pores, and the remaining coefficients are given by

$$D_K = \frac{2\epsilon r}{3\tau}\left(\frac{8RT}{\pi M}\right)^{1/2} \tag{3}$$

$$D_M = \frac{\epsilon}{\tau}PD \tag{4}$$

where r is the pore size, ϵ is the fractional void volume, δ is the membrane thickness, τ is the pore tortuosity, R is the gas constant, M is the molecular mass of water, D is the water diffusion coefficient, T is the absolute temperature, and P is the total pressure.

According to Eq. 1, the MD flux is proportional to the transmembrane water-vapor pressure difference: $\Delta P'_v = P_v(T'_w) - P_v(T'_a)$. The water-vapor pressure at the water side of the membrane, $P_v(T'_w)$, can be written as follows (ASHRAE, 1993)

$$P_v(T'_w) = \exp\left(\frac{C_1}{T'_w} + C_2 + C_3T'_w + C_4T'^2_w + C_5T'^3_w + C_6\ln T'_w\right) \tag{5}$$

where C_1 to C_6 are constants whose values (being P_v expressed in kPa and T'_w in K) are the following: $C_1 = -5.8002206\times10^3$; $C_2 = -5.516256$; $C_3 = -4.8640239\times10^{-2}$; $C_4 = 4.1764768\times10^{-5}$; $C_5 = -1.4452093\times10^{-8}$; $C_6 = 6.5459673$.

The water-vapor pressure corresponding to the air side of the membrane $P_v(T'_a)$ can be written as a function of the total pressure, P, and the humidity ratio, ω. This last magnitude is defined for a given moist air sample as the quotient between the mass flow rate of water vapor, $\dot{m}_{wa}$, and the mass flow rate of dry air, $\dot{m}_a$ (ASHRAE, 1993)

$$P_v(T'_a) = \frac{\omega P}{\omega + 0.622} \tag{6}$$

The problem is that the humidity ratio varies along the module length. Nevertheless, this value may be related with the air flow rate, $\dot{m}_a$, and with the value of the humidity at the module inlet, ω_{in}, which is known (ASHRAE, 1993)

$$\omega = \omega_{in} + NA/\dot{m}_a \tag{7}$$

where A is the membrane surface.

Equations 1 and 5−7 permit us to write a second-degree

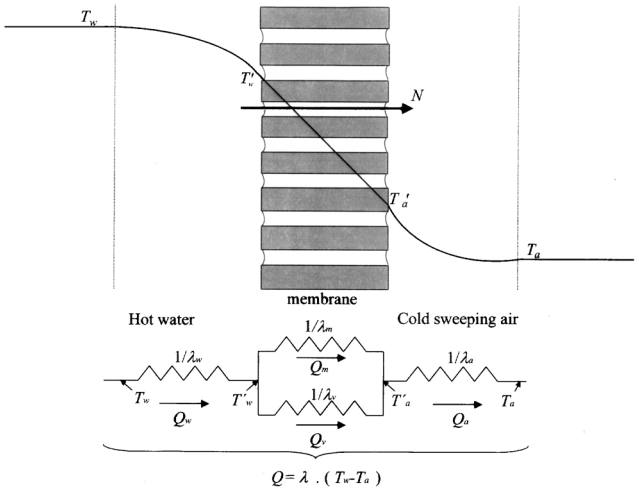

Figure 2. Temperature profile, heat fluxes, and heat-transfer resistances in SGMD.

equation for the transmembrane water flux, N

$$N^2 + uN + s = 0 \tag{8}$$

where the coefficients u and s are given by

$$u = (\omega_{in} + 0.622)\frac{\dot{m}_a}{A} + B'\left[P - P_v(T'_w)\right] \tag{9}$$

$$s = B'\frac{\dot{m}_a}{A}\left[P\omega_{in} - P_v(T'_w)(\omega_{in} + 0.622)\right] \tag{10}$$

It is well known that the heat-transfer mechanism in a MD process is usually depicted by means of a set of resistances (Lawson and Lloyd, 1997; Schofield et al., 1987) (see Figure 2). According to this idea, the heat fluxes through each of the resistances in Figure 2 are

$$Q = \lambda \cdot (T_w - T_a);\ Q_w = \lambda_w \cdot (T_w - T'_w);\ Q_a = \lambda_a \cdot (T'_a - T_a) \tag{11}$$

$$Q_m = \lambda_m \cdot (T'_w - T'_a);\ Q_v = \lambda_v \cdot (T'_w - T'_a) = N \cdot \Delta H_v \tag{12}$$

In these equations, Q is the overall heat flux; Q_w is the heat flux through the water chamber; Q_a is the heat flux through the air chamber; Q_m is the heat flux conducted through the membrane matrix; Q_v is the heat flux accompanying the MD flux; λ, λ_w, λ_a, λ_m, and λ_v are their associated heat transfer coefficients, respectively; and ΔH_v is the heat of vaporization of water. It is worth noting that, in steady state, the heat fluxes Q, Q_w, and Q_a are equal.

According to Lawson and Lloyd (1997), Khayet et al. (2000a), and Schofield et al. (1987), the overall heat-transfer coefficient for the process is

$$\lambda = \left[\frac{1}{\lambda_w} + \frac{1}{\lambda_m + (N \cdot \Delta H_v)/(T'_w - T'_a)} + \frac{1}{\lambda_a}\right]^{-1} \tag{13}$$

The conductive heat-transfer coefficient across the membrane (membrane matrix plus vapor entrapped in the pores) is

$$\lambda_m = \epsilon \cdot \lambda_{mg} + (1 - \epsilon) \cdot \lambda_{ms} \tag{14}$$

where λ_{mg} represents the conductive contribution of the air entrapped in the pores, and λ_{ms} is the contribution of the solid matrix.

In relation to the TP effects, it is well known that the temperatures in the bulk phases (T_w and T_a) are different from the values corresponding on the membrane surfaces (T'_w and T'_a). This phenomenon is usually quantified by means of the so-called "temperature polarization coefficient," θ, which is defined as

$$\theta = \frac{T'_w - T'_a}{T_w - T_a} = \frac{\Delta T'}{\Delta T} \tag{15}$$

In Khayet et al. (2000a), it was shown that this coefficient might be expressed as

$$\theta = 1 - \frac{\lambda}{\lambda_w} - \frac{\lambda}{\lambda_a} = 1 - \frac{\lambda}{\lambda_f} \tag{16}$$

where λ_f is the overall convective heat-transfer coefficient valid for both fluids

$$\lambda_f = \left(\frac{1}{\lambda_w} + \frac{1}{\lambda_a}\right)^{-1} \tag{17}$$

Equations 15–17 may be rearranged as

$$\theta = \theta_w + \theta_a - 1 \tag{18}$$

where the temperature polarization coefficients corresponding to the water and air phases are defined by

$$\theta_w = 1 - \frac{\lambda}{\lambda_w} = \frac{T'_w - T_a}{T_w - T_a} \tag{19}$$

$$\theta_a = 1 - \frac{\lambda}{\lambda_a} = \frac{T_w - T'_a}{T_w - T_a} \tag{20}$$

Figure 2 and Eqs. 11–13 suggest that the SGMD process is controlled by two simultaneous mechanisms: a mass transfer through the membrane, and a heat transfer through the composite system formed by the membrane plus the adjoining layers. Both mechanisms are interrelated. In principle four limit possibilities may occur:

1. If the heat transfer through the fluid phases is very large, the temperatures at the membrane surfaces approach the ones corresponding in the bulk phases. This means that the temperature polarization coefficient θ approaches unity (see Eq. 15). In this case, the temperature polarization effects are negligible and the mass-transfer resistance of the membrane controls the MD process.

2. If the heat transfer through the fluid phases is very small and the net MD coefficient is large, the difference between the temperatures at the membrane surfaces and the ones corresponding to the bulk phases is high, and the transmembrane temperature difference is low. This means that the temperature polarization coefficient θ approaches zero (see Eq. 15). In this case, the temperature polarization effects are very important and the heat-transfer resistances of the boundary layers control the MD process.

3. If the heat transfer through the sweeping air phase is very large, the temperature at the air-side membrane surface and the one corresponding to the bulk phase are very similar. This means that the air-temperature polarization coefficient θ_a approaches unity (see Eq. 20). In this case, Eq. 18 shows that the temperature polarization effects in the liquid phase are important, and the MD process is controlled by the heat-transfer resistance of the liquid layer and the mass-transfer resistance of the membrane.

4. If the heat transfer through the liquid phase is very large, the temperature at the water-side membrane surface and the one corresponding to the bulk phase are very similar. This means that the water temperature polarization coefficient θ_w approaches unity (see Eq. 19). In this case, the temperature polarization effects in the air phase are important. Therefore, the heat-transfer resistance of the air layer and the mass-transfer resistance of the membrane control the MD process.

In steady state, and assuming that the heat loss toward the exterior is negligible, the global heat flux, Q, can be calculated from the point of view of the global heat flux through the sweeping air, according to

$$Q_a = \frac{\dot{m}_a \cdot (h_{\text{aout}} - h_{\text{ain}})}{A} \tag{21}$$

where h_{aout} and h_{ain} are the specific air enthalpies at the module outlet and inlet, respectively. These parameters can be related to the humidity ratio as (ASHRAE, 1993; McAdams, 1964)

$$h_a = c_{ha} \cdot T_a + \omega \cdot \Delta H_v^{\bullet} = (c_a + \omega \cdot c_{wv}) \cdot T_a + \omega \cdot \Delta H_v^{\bullet} \tag{22}$$

where c_{ha} is the specific heat of the humid air, c_a is the specific heat of the dry air, c_{wv} is the specific heat of the water vapor, and $\Delta H_v^{\bullet}$ is the heat of vaporization of water at temperature 0°C. The problem is that the humidity ratio at the cell outlet is not known. Nevertheless, this value can be related to the value at the cell inlet, which is known, and the overall MD flux, N_{ov}, by using Eq. 7.

From Eqs. 7, 21, and 22 the following expression for the global heat flux through the air chamber is reached

$$Q_a = \frac{\dot{m}_a(c_a + \omega_{in} \cdot c_{wv}) \cdot (T_{\text{aout}} - T_{\text{ain}}) + N_{ov} \cdot A \cdot (\Delta H_v^{\bullet} + c_{wv} \cdot T_{\text{aout}})}{A} \tag{23}$$

A value for the global heat-transfer coefficient, λ, may be gotten by means of Eq. 11. It should be noted that we have used the log mean value $\Delta T_{\ln}$ for the temperature difference $\Delta T = T_w - T_a$. This last log mean value is defined as usual in single-pass counterflow heat exchangers (Kreith and Bohn, 1997)

$$\Delta T_{\ln} = \frac{\Delta T_0 - \Delta T_l}{\ln(\Delta T_0 / \Delta T_l)} \tag{24}$$

where ΔT_0 and ΔT_l are the temperature difference between liquid water and air bulk phases at the module inlet and outlet, respectively.

In addition, Eqs. 11–13 allow the transmembrane temperature difference for the whole system to be written as

$$\Delta T' = \frac{Q_a - N_{\text{ov}} \cdot \Delta H_v}{\lambda_m} \tag{25}$$

This equation can be transformed with the help of Eqs. 14, 15, 23 and 24 to get a global value for the temperature polarization coefficient

$$T = \frac{\dot{m}_a \cdot (c_a + \omega_{in} \cdot c_{wv}) \cdot (T_{\text{aout}} - T_{\text{ain}}) + N_{\text{ov}} \cdot A \cdot (\Delta H_v^{\bullet} + c_{wv} \cdot T_{\text{aout}})}{A \cdot \lambda_m \cdot \Delta T_{\ln}} \tag{26}$$

Due to the heat and mass transfer, which occur by evaporation and conduction across the membrane, temperature gradients are built up along the x and y coordinate in both chambers (see the coordinate system shown in Figure 1).

In order to determine the local temperature polarization, only a brief description of the theoretical model that develops the temperature profile in both fluids along the membrane module will be presented in this article. More details can be found in Khayet et al. (2000a).

As is well known, the temperature profile for both fluids is governed by the corresponding mass- and energy-balance equations. To get useful expressions for the dependence of the temperatures on the x and y coordinates, the following hypotheses are assumed:

(1) The system works in steady state.
(2) There is heat conduction along the y coordinate only.
(3) There is heat convection along the x coordinate.
(4) There are temperature gradients along the x and y coordinates, but not along z the coordinate.

In the hot chamber, the water flow rate, $\dot{m}_w$, decreases along the cell length due to the transmembrane evaporation. This implies a decrease of $\dot{m}_w$ with the x coordinate. Consequently, the following relationship applies

$$d\dot{m}_w = -N \cdot dA = -N \cdot b \cdot dx \tag{27}$$

where b is the z dimension of the membrane module.

The energy balance in the hot chamber can be written as (Incropera and Dewitt, 1985; Bird et al., 1960)

$$\rho_w \cdot c_w \cdot v_w \cdot \frac{dT_w(x,y)}{dx} = k_w \cdot \frac{d^2T_w(x,y)}{dy^2} \qquad (28)$$

with the following experimental boundary conditions for the water temperature, $T_w(x,y)$:

1. The water temperature at the module inlet is $T_w(0,0) = T_{\text{win}}$.
2. The water temperature at the module outlet is $T_w(l,0) = T_{\text{wout}}$.
3. The energy (per unit surface and time) that passes through the membrane from the hot water to the cold air is

$$Q = -k_w \cdot \left|\frac{dT_w}{dy}\right|_{y=d} \qquad (29)$$

In these equations, ρ_w is the water density, c_w is the specific heat of water, k_w is its thermal conductivity, and d is the y-dimension of the liquid chamber.

In the cold sweeping air chamber, the transmembrane water flux (N) incorporates to the air and increases the humidity ratio (ω). In this case, the water vapor carried by the sweeping air varies along the x coordinate, according to

$$d\dot{m}_{wa} = \dot{m}_a \cdot d\omega = -N \cdot dA = -N \cdot b \cdot dx \qquad (30)$$

The minus sign in Eq. 30 means that the humidity ratio increases when the x coordinate decreases.

The energy lost by the hot water is gained for the air. This process gives rise to an increase in the air enthalpy, h_a

$$\frac{\dot{m}_a}{b} \cdot \frac{dh_a}{dx} = -\lambda \cdot (T_w - T_a) \qquad (31)$$

with the following boundary conditions

For $x = 0$

$$\Delta T = T_{\text{win}} - T_{\text{aout}} = \Delta T_0 \qquad (32)$$

For $x = l$

$$\Delta T = T_{\text{wout}} - T_{\text{ain}} = \Delta T_l \qquad (33)$$

It is worth noting that in Eq. 31 the enthalpy of the moist air can be obtained from Eq. 22.

The resolution of the cited equations can be seen in detail in Khayet et al. (2000a). There, it was shown that the temperature profiles were as follows:

$$T_w(x) = T_{\text{win}}\left(\frac{T_{\text{wout}}}{T_{\text{win}}}\right)^{x/l} \approx T_{\text{win}} + \frac{T_{\text{wout}} - T_{\text{win}}}{l}x \qquad (34)$$

$$T'_w(x) = T_w(x)\frac{1}{\cos(\beta d)} - \frac{Qtg(\beta d)}{k_w \beta} \qquad (35)$$

$$T_a(x) = T_w(x) - \left(\Delta T_l - \frac{T_{\text{wout}} - T_{\text{win}}}{l\alpha}\right) \times \exp\left[\alpha(l-x)\right] - \frac{T_{\text{wout}} - T_{\text{win}}}{l\alpha} \qquad (36)$$

$$T'_a(x) = T'_w(x) - \frac{\lambda - B\dfrac{dP}{dT}\Delta H_v}{\lambda_m}\left[T_w(x) - T_a(x)\right] \qquad (37)$$

In Eqs. 35 and 36, the new unknown parameters are given by

$$\beta^2 = \frac{\rho_w c_w v_w}{lk_w} \ln\left(T_{\text{win}}/T_{\text{wout}}\right) \qquad (38)$$

$$\alpha = \left\{\left[\lambda - \lambda_m\left(1 - \frac{\lambda}{\lambda_f}\right)\right]\frac{\Delta H_v^{\bullet}}{\Delta H_v} - \lambda\right\}\frac{b}{\dot{m}_a c_{ha}} \qquad (39)$$

Consequently, Eq. 8 has been solved numerically and theoretical values of the local MD flux $N(x)$ have been obtained. From these local fluxes, the global fluxes for the complete membrane module are obtained according to

$$N_{\text{ov}} = \frac{1}{l}\int_0^l N(x)\,dx \qquad (40)$$

Otherwise, from Eqs. 34–37, a new coefficient termed "local temperature polarization coefficient, $\theta(x)$" has been defined. From this local coefficient, the global one corresponding to the whole membrane module can be calculated using a procedure analogous to the one expressed in Eq. 40

$$T = \frac{1}{l}\int_0^l \theta(x)\,dx = \frac{1}{l}\int_0^l \frac{T'_w(x) - T'_a(x)}{T_w(x) - T_a(x)}dx \qquad (41)$$

In this way, the global temperature polarization coefficient, Θ, can be calculated from the local temperature polarization values by means of Eq. 41, or alternately, from Eq. 26. Obviously, if the theory developed in this section is correct, the values obtained by the two methods must be similar. This fact will be discussed in the next section.

From Eqs. 19 and 20, local temperature polarization coefficients for the water, θ_w, and air, θ_a, phases have been defined separately. A global water temperature polarization coefficient, Θ_w, as well as a global air temperature polarization coefficient, Θ_a, can be calculated in an analogous way, as in Eq. 41.

Results and Discussion

The main aim of this work is to analyze the temperature polarization effects in both fluid phases separately. The SGMD setup described in the experimental part permits liquid water and sweeping air to be circulated at each side of the membrane module. The circulation velocity and the inlet temperature of both fluids can be controlled independently.

In all the experiments, a temperature gradient is built along the membrane module (Khayet et al., 2000a,b). This affects the local driving force and, consequently, the MD flux. With

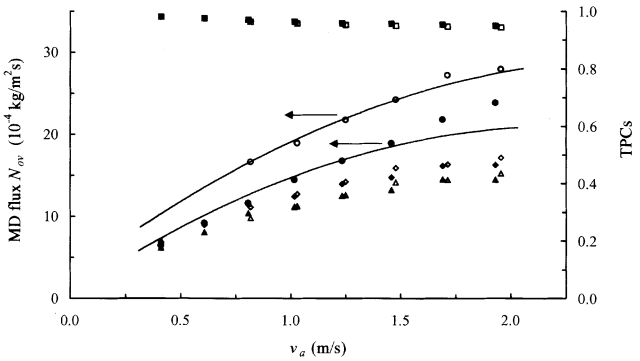

Figure 3. MD flux, N_{ov}, and calculated global temperature polarization coefficients (TPCs) vs. sweeping air velocity.

Membrane TF-200 [N_{ov} (●); Θ (▲); Θ_a (♦); Θ_w (■)] and membrane TF-450 [N_{ov} (○); Θ (△); Θ_a (◇); Θ_w (□)], with $v_w = 0.15$ m/s, $T_{ain} = 20$°C, and $T_{win} = 50$°C; the solid lines represent the fit according to the combined Knudsen/molecular diffusion model (Eq. 2).

this in mind, in all the studied cases, the global values for the whole MD system corresponding to each parameter, MD flux, or temperature polarization coefficients have been calculated, and the results corresponding to some particular cases are shown in Figs. 3–6. It must be pointed out that the error bars corresponding to each point have not been shown, because they are approximately equal to the size of the dotted points ($\leq 4\%$).

In what follows, the effects of the different operating parameters will be discussed separately.

The effect of the air circulation velocity on the MD flux for both membranes is shown in Figure 3. The data shows the same general trend in both membranes. The MD flux is greater (within 14% to 30%) in the case of the membrane TF-450 than in that of the membrane TF-200. Similarly, the theoretical values of the net MD coefficient, calculated from Eq. 2, are greater (within 25% to 31%) in the case of the membrane TF-450 than in the membrane TF-200. This fact is associated with the different pore radii.

The solid lines depicted in this figure show the theoretical curves corresponding to the overall MD flux obtained from the combined Knudsen/molecular diffusion model. It is worth mentioning that the main uncertainty in MD processes is the tortuosity factor of the membrane pores. The influence of this parameter for these membranes was discussed in a previous paper (Khayet et al., 2000b). There, a value of 1.1 was estimated to be adequate. The figure shows that the agreement between the theoretical predictions and the experimental data over the air velocity range investigated can be considered good (it is at least 13% for the membrane TF-200 and 5% for the membrane TF-450).

A visual inspection of the experimental data in Figure 3 permits us to state that the MD flux increases with the air circulation velocity due to changes in the Reynolds numbers. As a matter of fact, these numbers, calculated for the air chamber according to Lawson and Lloyd (1997), range from 741 to 3,644 for membrane TF-200 and from 1,482 to 3,634 for membrane TF-450. The TPCs corresponding to the water and air phases, as well as the overall one, were quantified according to the proposed analysis mentioned in the theory section. Figure 3 shows the obtained values for TF-200 and TF-450, respectively. Note that the presented TPCs are the global values along the membrane module, and they have been evaluated from Eq. 41 by means of the local TPCs. In order to check the consistency of the proposed theoretical model, the global temperature coefficient of the whole system, Θ, was calculated with the help of the two methods proposed previously, Eqs. 26 and 41. In this particular case, the discrepancy between both values of Θ was 4% in the most unfavorable case.

The same trends were observed in Figure 3, which means that the TP effects are similar for both membranes. This fact is not unexpected if one takes into account that the TP effects depend mainly on the dynamical properties of the fluids adjoining the membrane, rather than on the membrane characteristics. The overall TPC, Θ, and the air TPC, Θ_a, both increase with the air circulation velocity. On the other hand, the water TPC, Θ_w, hardly varies at all. Note that the global TPC, Θ, is lower than 0.5. This means that more than 50% of the externally applied thermal driving force is dissipated in the unstirred layers. Nevertheless, the value of Θ_w is very close to unity, which means that the effect of the water temperature polarization is very low. However, the value of the air TPC, Θ_a, is lower than 0.5 and is very close to the corresponding global TPC, Θ. This result can be clarified by studying the overall heat-transfer coefficient, which includes the heat-transfer coefficients in the water and the air sides. As an example, in the particular case of the operating conditions described in Figure 3, when the air circulation velocity was increased from 0.8 to 2 m/s, the overall heat-transfer coefficient increased from 311 to 425 W/m$^2 \cdot$ K for membrane TF-200 and from 336 to 513 W/m$^2 \cdot$ K for membrane TF-450. It is worth noting that the heat-transfer coefficient in the water side is more than 10 times higher than the heat-transfer coefficient in the air side. This result may be interpreted by saying that the overall heat-transfer coefficient is dominated by the sweeping air contribution (see Eqs. 13 and 17). Therefore, the air TPC is the dominant parameter in the SGMD process. In order to be sure, more tests have been carried out at different water inlet temperatures for both membranes. The same conclusion is always obtained.

As a consequence, in SGMD experiments, an increase in the air circulation velocity is accompanied by a decrease in the TP effects and, consequently, by an increase in the MD flux.

On the other hand, it is worth noticing that the temperature drop observed between the inlet and outlet of the membrane module in both fluid phases changes with the air circulation velocity, being very high in the case of the air phase. The decrease in the water temperature along the membrane module ranges between 0.2% and 0.6%, for both membranes, whereas the increase of the air temperature is higher than 76%. This fact was discussed in detail in Khayet et al. (2000a).

Figure 4 shows the MD flux as a function of the water circulation velocity for both membranes. The solid lines correspond to the theoretical curves obtained according to the combined Knudsen/molecular diffusion model. A visual inspection permits us to say that the agreement between theory and the experiments seems good. On the other hand, the solid lines seem to be practically horizontal. In order to be more

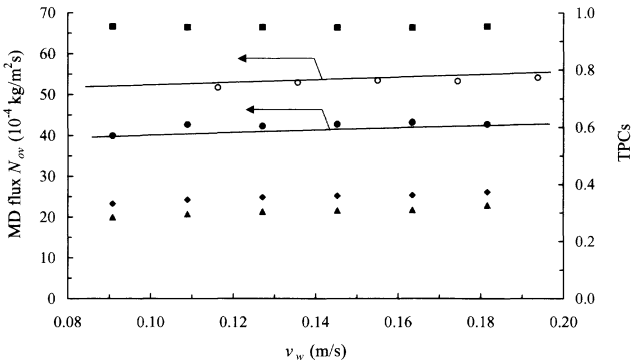

Figure 4. MD flux, N_{ov}, [TF-200 (●) and TF-450 (○)] and calculated global temperature polarization coefficients (TPCs), for membrane TF-200. Θ (▲); Θ_a (♦); Θ_w (■) vs. the water circulation velocity.

$v_a = 1.5$ m/s, $T_{ain} = 20$°C, and $T_{win} = 65$°C; solid lines represent the fit according to the combined Knudsen/molecular diffusion model (Eq. 2).

rigorous, the probability of a zero slope has been calculated by means of data analysis. The pairs of experimental data points $\{N_{ov};v_w\}$ have been adjusted to a horizontal line by using a least-square procedure. The calculated probability of a zero slope is always greater than 91% for both membranes. This result reasonably permits us to state that the MD flux is practically independent of the water circulation velocity in the range of experimental conditions under investigation.

This practical independence of the MD flux on the water circulation velocity is, at first sight, rather surprising. An examination of the literature devoted to MD (see, for example, Lawson and Lloyd, 1997) predicts that both magnitudes are related. An increase in the water-circulation velocity should lead to an increase in the MD flux that asymptotically approaches a value when the turbulent flow regime is reached. This fact is due to the increase of the Reynolds number, which is proportional to the fluid circulation velocity, leading to an increase in the heat-transfer coefficient in the boundary layer near the membrane surface, thus, producing a reduction in the TP effect.

As is well known (Incropera and Dewitt, 1985; Bird et al., 1960), the value of the Reynolds number defines the regime of the flux. In the present case, the calculated Reynolds number in the water chamber varies between 3512 and 8814 for both membranes. This means that, in the range considered, the flow regime corresponds to a laminar–turbulent to turbulent transition. It is worth mentioning that, due to the experimental conditions, it was not possible to increase the water circulation velocity through the membrane module. In fact, if the water-circulation velocity is increased, the liquid feed pressure would be increased, and the risk of membrane wetting would become higher. Therefore, we conclude that the MD flux has reached a limiting value over the water-circulation velocities studied.

Moreover, the trends observed in Figure 4 can be better understood by studying the TP effect. As in the case of the experiments with varying air velocity, the global TPCs corresponding to the water and air phases, Θ_w and Θ_a, as well as the overall one, Θ, were calculated. The values obtained for the membrane TF-200 are presented in Figure 4. It is worth noting that the membrane TF-450 shows a similar trend.

Figure 4 shows that neither the MD flux nor the TPCs are affected significantly by the water-circulation velocity. The same behavior has been observed for other water inlet temperatures and other air-circulation velocities.

Note that the overall TPC for both membranes is still smaller than 0.5 in the entire velocity range. This means that the mass transport is predominantly controlled by heat transfer through the boundary layers adjacent to the membrane surfaces. Otherwise, the water TPCs are near 1 over the entire investigated water-circulation velocity range, and the air TPCs differ only by 13% from the overall TPCs. This means that most of the TP is located in the air phase, and, thus, the mass flux in the SGMD process is almost completely controlled by the heat transfer through the air boundary layer.

From the point of view of the continuity of the heat flow, it was checked that the heat transferred from the water to air phases is not influenced appreciably by the water-circulation velocity. In this particular case (see Figure 4), the overall heat-transfer coefficient is about 420 W/m^2 K for membrane TF-200, and 499 W/m^2 K for membrane TF-450. It should be pointed out that the larger MD flux obtained with the TF-450 membrane involves a larger heat flux. In this case, the heat-transport flux is dominated by the resistance generated in the air boundary layer, especially at a low air circulation velocity. In other words, under the operating conditions presented in Figure 4, the contribution of the air TP effect is about 93%, for both membranes. It must be noticed that if it were assumed that the SGMD process had been carried out by ignoring the TP effect on the water side, the predicted MD fluxes would have been 19% higher than those calculated taking the water TP effect into account.

Figure 5 shows the negative influence of the air-inlet temperature on the MD flux for both membranes. As in the previous figures, the solid lines correspond to the theoretical curves obtained for a combined Knudsen/molecular diffusion transport. Once again, it can be observed that the theoretical curves fit the experimental data closely. Similar figures might be drawn under the various experimental conditions studied throughout this article.

The observed decrease in the measured fluxes with the air-inlet temperature can be easily explained if one takes into account that an increase in the sweeping air temperature produces a decrease in the transmembrane temperature difference and, consequently, in the vapor-pressure gradient, which is the driving force for the MD process.

In all cases, the decrease in the MD flux with the air-inlet temperature is linear with a correlation coefficient greater than 0.98. The slopes of the straight lines in Figure 5 are about 40%, for the TF-200 membrane, and 39%, for the TF-450 membrane when the air-inlet temperature varies from 10°C to 30°C. This means that the effect of the air-inlet temperature on the MD flux is not negligible. This result is not in agreement with the one reported in Basini et al. (1987).

According to the previous discussion, it seems that the heat transfer through the air boundary layer controls the mass transport in the range of circulation velocities studied. In order to confirm this conclusion, the global TPCs will be evaluated as function of the air-inlet temperature. The results corresponding to the TF-450 membrane, can be seen in Figure

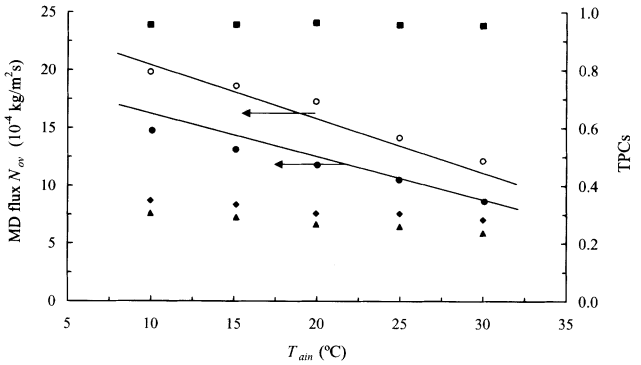

Figure 5. MD flux, N_{ov}, [TF-200 (●) and TF-450 (○)] and calculated global temperature polarization coefficients (TPCs) for membrane TF-450 Θ (▲); Θ_a (♦); Θ_w (■) vs. the water circulation velocity.

$v_a = 1.5$ m/s, $T_{ain} = 20$°C, and $T_{win} = 65$°C; solid lines represent the fit according to the combined Knudsen/molecular diffusion model (Eq. 2).

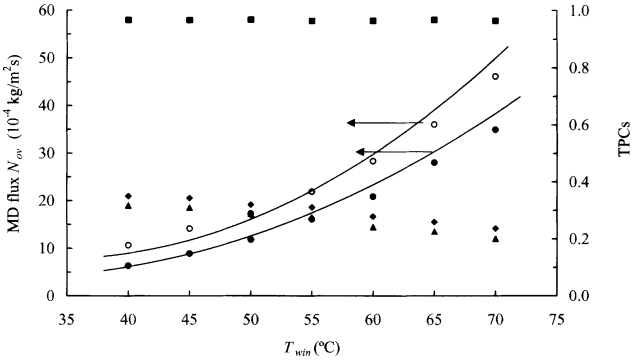

Figure 6. MD flux, N_{ov}, [TF-200 (●) and TF-450 (○)] and calculated global temperature polarization coefficients (TPCs) for membrane TF-200 Θ (▲); Θ_a (♦); Θ_w (■) vs. the water circulation velocity.

$v_a = 1.5$ m/s, $T_{ain} = 20$°C, and $T_{win} = 65$°C; solid lines represent the fit according to the combined Knudsen/molecular diffusion model (Eq. 2).

5. The same trend was observed with the TF-200 membrane and other experimental conditions.

As shown, changes in the air temperature did not affect the water TPC that is maintained near unity. However, an increase in the air-inlet temperature was accompanied by a slight decrease in the air TPC and a corresponding reduction in the overall TPC ($< 17\%$). We should point out that, in other MD experiments the polarization effects become more important as the cooling temperature increases (Lawson and Lloyd, 1997; Khayet et al., 2000a).

The decrease in the MD flux observed as the air-inlet temperature increases is related to a decrease in the heat flux through the fluid phases and in the temperature gradient in the boundary layers. Besides, lower global TPCs were achieved ($\Theta < 0.4$) even if the air-inlet temperature was varied in 20°C, say, from 10 to 30°C. Therefore, the MD transport is controlled by heat transfer, especially through the air boundary layer, as the heat-transfer coefficient through the liquid phase is very large in comparison with the heat-transfer coefficient in the air phase.

Moreover, if one considers that the TP is a measure of the relative effect of the heat transfer, it was confirmed that changes in the air inlet temperature have very little effect on the heat-transfer coefficients. In fact, the increase of the air inlet temperature from 10°C to 30°C implies a variation in the overall heat-transfer coefficient of at most 4% for both membranes. This may be due to the fact that in these series of experiments the water and air circulation velocities were maintained constant, and consequently the fluid-flow regimes are not altered. As shown in Figures 3 and 5, the MD fluxes are affected more by the air circulation velocity than by the air temperature. This fact corroborates that the flux is controlled by heat-transfer resistance.

As a summary, an increase in the air-inlet temperature causes an increase in the overall TP effects and a decrease in the MD flux.

Figure 6 shows the influence of the water-inlet temperature on the MD flux for both membranes. As earlier, the solid lines refer to the combined Knudsen/molecular diffusion model. The agreement between the model predictions and the experimental data is good.

As it is well known, in the MD process the feed temperature is the operating variable that affects more significantly the permeate flux. This is due to the exponential dependence of the water-vapor pressure on temperature (Lawson and Lloyd, 1997).

Equation 5 predicts an exponential increase in the vapor pressure with the temperature. This implies a similar dependence between the MD flux and the water-inlet temperature (see Figure 6). Note that, due to the additional effect of the TP previously cited, the MD flux does not increase with the water temperature as fast as the vapor pressure curve. This result agrees with those reported previously by means of VMD, DCMD, and AGMD (Lawson and Lloyd, 1997; Gryta and Tomaszewska, 1998; Vázquez-González and Martínez, 1994; Schofield et al., 1987; Ortiz de Zárate et al., 1990).

To confirm this fact, the global TPCs have been calculated as indicated in the previous section. Representative results for the TF-200 membrane, are shown in Figure 6 where one can see that the coefficient Θ_w remains constant with the water-inlet temperature, while the coefficients Θ and Θ_a decrease from 0.4 to 0.2. Similar trends have been observed for the TF-450 membrane. The contribution of the water TP effect is about 5%, for both membranes in the entire water-temperature range investigated. These results permit us to state that the TP is an important factor affecting the mass flux, and that the air boundary layer exerts the greatest effect in the SGMD process. In other words, the heat-transfer coefficient in the liquid phase is very large, and the fourth limit possibility proposed in the Theory section takes place.

It is worth noticing that two opposite contributions are taking place simultaneously. An increase in the water inlet temperature implies an increase in the TP effect, but also an increase in the MD flux. As heat is removed from the feed to vaporize the permeate, the temperature in the liquid–membrane interface decreases and the air temperature increases. This implies a decrease in the driving temperature difference, leading to a decrease in the water-vapor pressure gradi-

ent and a corresponding reduction in the MD flux. Nevertheless, the increase in the water-inlet temperature by steps of 5°C in each experimental run, overcomes the influence of the TP.

In addition, note that in this set of experiments, both circulation velocities are maintained constant and the effect of the air temperature is small. In this case, a temperature change at high water temperature implies a larger change in partial vapor pressure than the same change at low water temperature. For example, a temperature drop of 0.1°C at a temperature of about 30°C results in a variation in the vapor pressure of approximately 24.4 Pa, whereas at 70°C, the vapor pressure changes by 135 Pa.

To conclude, the heat transfer through the cell that contributes to the observed behavior shown in Figure 6 must be emphasized. In this particular case, over the water temperature interval studied (40–70°C), the overall heat-transfer coefficient increases about 21.8% and 22.9% for the TF-200 and TF-450 membranes, respectively. On the other hand, the trends in the heat-transfer coefficients in the water and air sides are not so clear at the high water-inlet temperature. This is probably due to the heat loss to the surroundings. Nevertheless, one might expect a slight decrease in these coefficients with temperature from the well-known empirical heat-transfer correlations usually used in the MD literature for laminar or turbulent flow regimes.

Conclusions

A new theoretical approach has been developed to analyze the TP effects in the case of the SGMD processes. The effects of the relevant operating parameters on the permeate flux and on the TPCs have been studied. The most important conclusions are:

- All the experimental results have been satisfactorily interpreted on the basis of the combined Knudsen/molecular diffusion model.
- The global TPC of the whole system was calculated with the help of two methods. The agreement was good.
- An increase in the air-circulation velocity gives rise to a decrease in the TP effects, and consequently, to an increase in the MD flux.
- In the range of experimental conditions investigated, the MD flux and the TPCs are not affected significantly by the water-circulation velocity.
- An increase in the air temperature was accompanied by an increase in the overall TP effects and a decrease in the MD flux.
- The MD flux increases exponentially with the water-inlet temperature in spite of the increase in the TP effect.
- The TP is an important factor affecting the mass flux in the SGMD process. In the range studied, the global TPC is lower than 0.5, which means that more than 50% of the external driving force is dissipated in the boundary layers adjoining the membrane surfaces.
- Under the experimental conditions studied in this work, the value of the water TPC remains very close to unity. This means that the main TP is located in the air phase, and the mass flux in the SGMD process is mostly controlled by the heat transfer through the air boundary layer.

Acknowledgments

Economical support from the CICYT is acknowledged.

Literature Cited

ASHRAE, *Fundamentals-Handbook, American Society of Heating, Refrigerating and Air-Conditioning Engineers*, New York (1993).

Basini, L., G. D´Angelo, M. Gobbi, G. C. Sarti, and C. Gostoli, "A Desalination Process Through Sweeping Gas Membrane Distillation," *Desalination*, **64**, 245 (1987).

Bird, R. B., W. E. Stewart, and E. N. Lightfoot, *Transport Phenomena*, Wiley, New York (1960).

Chmielewski, A. G., G. Zakrzewska-Trznadel, N. R. Miljevic, and W. A. Van Hook, "Membrane Distillation Employed for the Separation of Water Isotopic Compounds," *Sep. Sci. Technol.*, **30**(7–9), 1653 (1995).

Drioli, E., and Y. Wu, "Membrane Distillation: An Experimental Study," *Desalination*, **53**, 339 (1985).

Franken, A. C. M., J. A. M. Nolten, M. H. V. Mulder, D. Bargeman, and C. A. Smolders, "Wetting Criteria for the Applicability of Membrane Distillation," *J. Memb. Sci.*, **33**, 315 (1987).

Godino, M. P., L. Peña, and J. I. Mengual, "Membrane Distillation: Theory and Experiments," *J. Memb. Sci.*, **121**, 83 (1996).

Gryta, M., and M. Tomaszewska, "Heat Transport in the Membrane Distillation Process," *J. Memb. Sci.*, **144**, 211 (1998).

Incropera, F. P., and D. P. Dewitt, *Introduction to Heat Transfer*, Wiley, New York (1985).

Khayet, M., M. P. Godino, and J. I. Mengual, "Theory and Experiments on Sweeping Gas Membrane Distillation," *J. Memb. Sci.*, **165**, 261 (2000a).

Khayet, M., M. P. Godino, and J. I. Mengual, "Nature of Flow in Sweeping Gas Membrane Distillation," *J. Memb. Sci.*, **170**, 243 (2000b).

Kreith, F., and M. S. Bohn, *Principles of Heat Transfer*, PWS, Boston (1997).

Lawson, K. W., and D. R. Lloyd, "Membrane Distillation," *J. Memb. Sci.*, **124**, 1 (1997).

McAdams, W. H., *Transmisión de Calor*, Del Castillo, Madrid (1964).

Ortiz de Zárate, J. M., F. García-López, and J. I. Mengual, "Temperature Polarization in Non-Isothermal Mass Transport Through Membranes," *J. Chem. Soc. Faraday Trans.*, **86**(16), 2891 (1990).

Peña, L., J. M. Ortiz de Zárate, and J. I. Mengual, "Steady States in Membrane Distillation: Influence of Membrane Wetting," *J. Chem. Soc. Faraday Trans.*, **89**(24), 4333 (1993).

Sarti, G. C., C. Gostoli, and S. Matulli, "Low Energy Cost Desalination Processes Using Hydrophobic Membranes," *Desalination*, **56**, 277 (1985).

Schofield, R. W., A. G. Fane, and C. J. D. Fell, "Heat and Mass Transfer in Membrane Distillation," *J. Memb. Sci.*, **33**, 299 (1987).

Schofield, R. W., A. G. Fane, and C. J. D. Fell, "Gas and Vapor Transport Through Microporous Membranes I and II," *J. Memb. Sci.*, **53**, 159 (1990).

Vázquez-González, M. I., and L. Martínez, "Water Distillation Through PTFE Hydrophobic Membranes," *J. Chem. Soc. Faraday Trans.*, **90**, 2043 (1994).

Manuscript received Oct. 18, 2000, and revision received Dec. 6, 2001.